Colloids and Surfaces B: Biointerfaces 82 (2011) 513–517

Contents lists available at ScienceDirect

Colloids and Surfaces B: Biointerfaces

journal homepage: www.elsevier.com/locate/colsurfb

Preparation and characterization of silver nanoparticles by chemical reduction method

Zaheer Khan*, Shaeel Ahmed Al-Thabaiti, Abdullah Yousif Obaid, A.O. Al-Youbi

Department of Chemistry, Faculty of Science, King Abdul Aziz University, P.O. Box 80203, Jeddah 21413, Saudi Arabia

ARTICLE INFO

Article history:
Received 10 July 2010
Accepted 5 October 2010
Available online 12 October 2010

Keywords:
Silver nanoparticles
Chemical reduction
CTAB
Surface plasmon
Silver(I)

ABSTRACT

Silver nanoparticles were prepared by the reduction of $AgNO_3$ with aniline in dilute aqueous solutions containing cetyltrimethlyammonium bromide, CTAB. Nanoparticles growth was assessed by UV–vis spectroscopy and the average particle size and the size distribution were determined from transmission electron microscopy, TEM. As the reaction proceeds, a typical plasmon absorption band at 390–450 nm appears for the silver nanoparticles and the intensities increase with the time. Effects of [aniline], [CTAB] and [Ag^+] on the particle formation rate were analyzed. The apparent rate constants for the formation of silver nanoparticles first increased until it reached a maximum then decreased with [aniline]. TEM photographs indicate that the silver sol consist of well dispersed agglomerates of spherical shape nanoparticles with particle size range from 10 to 30 nm. Aniline concentrations have no significant effect on the shape, size and the size distribution of Ag-nanoparticles. Aniline acts as a reducing as well as adsorbing agent in the preparation of roughly spherical, agglomerated and face-centered-cubic silver nanoparticles.

1. Introduction

Preparation and characterization of novel nanostructures (cubes, disks, plates, prisms, triangles, wires, rods and macroporous) of noble metals, silver and gold, have come a long way of various investigators in many laboratories[1–5] and their uses in photography, catalysis, biological labeling, superconductors, photonics, optoelectronics, super magnets, surface-enhanced Raman scattering detection, environment, sensors, antimicrobial and antibacterial activities, etc. are unlimited [6–10]. Method of preparation (radiation, chemical, photochemical, and electrochemical) [11–15] and experimental conditions such as [reactants], [stabilizer and/or capping agents], pH, temperature, order of mixing of reactants, presence of nucleophilic and electrophilic reagents, nature of stabilizers and capping agents and even the rate of addition of reducing agents are the important parameters which control the size, morphology, shape, stability, color, and physicochemical properties of the advanced nanomaterials [16–20]. Chemical reduction is the most frequently applied method for the preparation of stable silver nanoparticles and its colloidal dispersions in water or organic solvents [21–23].

Henglein et al. monitored the stepwise growth of silver clusters in aqueous solution by spectroscopic methods and suggested that the small metal particles in solution have been found advantageous over the water-insoluble forms because UV–vis spectrophotometer can be used to monitor the optical changes that accompany the surface reactions [11,24,25]. Generally, sodium borohydride, hydrazine, ascorbic acid and cetyltrimethylammonium bromide, sodiumdodecyl sulphate, poly(vinyl alcohol), poly(vinylpyrrolidone), are used as the reducing- and stabilizing-agents, respectively, to prepare shape- and size-controlled silver nanocrystals. The chemical reduction methods are probably the most versatile, economical and easy to control the shape and size of metal nanoparticles.

Chaudret and his coworkers reported a classical method to the preparation of gold nanoparticles by using long chain primary amines ($C_nH_{2n+1}NH_2$; n = 8, 12, 16) as stabilizers [26]. Poly(amidoamine) dendrimers with surface –NH_2, –OH and –COOH groups have been used as the protective colloid for the preparation of dendrimer-encapsulated gold and silver nanoparticles by the photo radiation and chemical reduction methods [27,28]. Esumi et al. [29] used sugar-persubstituted poly (amidoamine) as the reducing and stabilizing agent for the preparation of gold and silver nanoparticles in aqueous solution and suggested that the hydroxyl groups of glucose residues of sugar ball operate as reduction sites for Ag^+ ions in alkaline medium. Out of these groups, –NH_2 has strong affinity towards the metal surfaces.

Li and co-workers used hydrazine hydrate and sodium citrate for the reduction of Ag^+ ions in presence of aniline and reported a method to the preparation of aniline-derivatized silver nanocrystals of different morphologies [30]. Aniline is one of the most serious

* Corresponding author. Permanent address: Department of Chemistry, Jamia Millia Islamia (Central University), New Delhi 110025, India.
E-mail address: drkhanchem@yahoo.co.in (Z. Khan).

0927-7765/$ – see front matter © 2010 Elsevier B.V. All rights reserved.
doi:10.1016/j.colsurfb.2010.10.008

environmental contaminants and weak reducing agent; reduction potential = 0.45 V at Ag/AgCl; it is released in the environment after its use in the manufacturing of dyes, rubber, polymers, herbicides, pesticides, fungicides and pharmaceuticals [31]. It is also in the effluents of coal liquefaction [32]. Biological, chemical and photochemical methods [33–35] have been used for the removal of this pollutant. It is believed that redox chemistry of aniline plays an important role in the protection of environment The silver particles may be useful, in favorable situations, investigating the oxidative degradation of –N, –O and –S containing toxic organic compounds by silver sol by passing the problems arising from the precipitation of Ag^0. To the best of our knowledge, there are no reports about the use of aniline as the reductant in the growth of surfactant-induced anisotropic silver nanoparticles. In this work we focus, for the first time, on the effect of [aniline], [CTAB] and [Ag^+] to the reduction of Ag^+ ions by aniline.

2. Experimental

2.1. Chemicals and instruments

All glassware was thoroughly cleaned prior to use with freshly prepared aqua regia (HCl:HNO_3 = 3:1) and rinsed with double-distilled, CO_2-free, and deionized water. Aniline, Ph–NH_2 (reductant, 99.9%, BDH) was purified by distillation under a stream of nitrogen gas free from O_2 gas before use. Silver nitrate (oxidant, 99.9%, BDH), cetyltrimethylammonium bromide (98%, Fluka) were used as received without further purification. Distilled water was used as solvent to prepare all the solutions in this study. The UV–vis absorption spectra were taken at room temperature on a Spectrophotometer, UV-260 Shimadzu, with a variable wavelength between 375 and 750 nm using a 1 cm quartz cuvettes of optical path. Transmission electron microscopic micrographs and selected area electron diffraction (SAED) data were recorded on a TECHNAI-320KV (JAPAN), Model No. Ultra Twin SEI with EDAXJEOL, electron microscope operating at 80 kV. Samples were prepared by placing a drop of working solution on a carbon-coated standard copper grid (300 mesh), which was air dried before making the TEM measurement. Fisher Scientific digital pH meter 910 fitted with a combination electrode was used for pH measurements. The Fourier transform infrared (FT-IR) spectra experiments were carried out on a Bruker Equinox 55 spectrophotometer. A few drops of the resulting sol were placed on a KBr pellets and allowed to dry IR spectra recorded.

2.2. Preparation of Ag-nanoparticles

Silver nanoparticles were prepared by the reduction of silver nitrate solution with aniline in presence of CTAB. A series of experiments were performed, varying the concentration of oxidant, reductant and stabilizer to obtain a perfectly transparent silver sol. In a typical procedure, 8 ml of a 0.01 mol dm^{-3} solution of silver nitrate was mixed with 5 ml of a 0.01 mol dm^{-3} CTAB solution. The colorless reaction mixture was slowly converted to the characteristic pale yellow color, when 20 ml of a 0.01 mol dm^{-3} solution of aniline was added in the solution of silver nitrate and CTAB. The total volume of the reaction mixture was always 50 ml. The whole solution had a pH of 10.2. The appearance of color was indicated the formation of Ag-nanoparticles [10,11].

2.3. Rate measurement of Ag-nanoparticles formation

The required volume of $AgON_3$ and CTAB was taken in a two-necked reaction vessel equipped with a double-surface condenser to prevent evaporation. The reaction vessel was kept immersed in the water bath thermostated at room temperature and the solution was left to stand for 5 min to attain equilibrium. The reaction was initiated with the addition of required volume of aniline solution. The zero time was taken when half of the aniline solution has been added. The progress of the reaction was followed spectrophotometrically by pipetting out aliquots at definite time intervals and measuring the absorbance of silver sol formation (pale-yellow color; λ_{max} = 400 nm *vide infra*) with a spectrophotometer. In the present study, the kinetic runs were carried out as a function of [CTAB] (2.0×10^{-4} to 40.0×10^{-4} mol dm^{-3}), [Ag^+] (2.0×10^{-4} to 50×10^{-3} mol dm^{-3}), [aniline] (2.0×10^{-4} to 40.0×10^{-4} mol dm^{-3}). The apparent rate constants (k_{obs}, s^{-1}) were calculated from the initial part of the slopes of the plots of $\ln(a/(1-a))$ *versus* time with a fixed time method [12]. Duplicate runs gave results that were reproducible to within ±5%. Other details of kinetic procedure were the same as described previously [20]. The pH of the reaction mixture was also measured at the end of each kinetic experiment and observed that pH drift during the course of the reaction is very small (within 0.04 unit).

3. Results and discussion

3.1. Characterization of Ag-nanoparticles

The selection of an appropriate reducing agent and selection of nontoxic stabilizer for the stability of Ag-nanoparticles is a crucial problem because size, shape and size distribution strongly depend on the nature of reducing and stabilizers [11]. Metal nanoparticles those were prepared by the mild reducing agents, was relatively more stable compared with those produced by excess of strong reducing agents [36]. Aniline is one of the relatively milder reductants used for the reduction of silver ions. We used CTAB to act as stabilizer. UV–vis spectra of an Ag sol recorded as a function of time and compilation of the absorbance are shown in Fig. 1. The increase in absorbance at 400 nm as a function of time can be seen. Plasmon absorption band with a λ_{max} at 400 nm is commonly presented as the characteristic of successful spherical or roughly spherical faceted Ag-nanoparticles synthesis. Fig. 2 shows TEM micrographs of Ag-nanoparticles prepared. It can be seen that the size of the roughly spherical nanoparticles ranges between 10 and 30 nm and their size distribution is relatively wide. Inspection of TEM images confirms thus the formation of CTAB stabilized

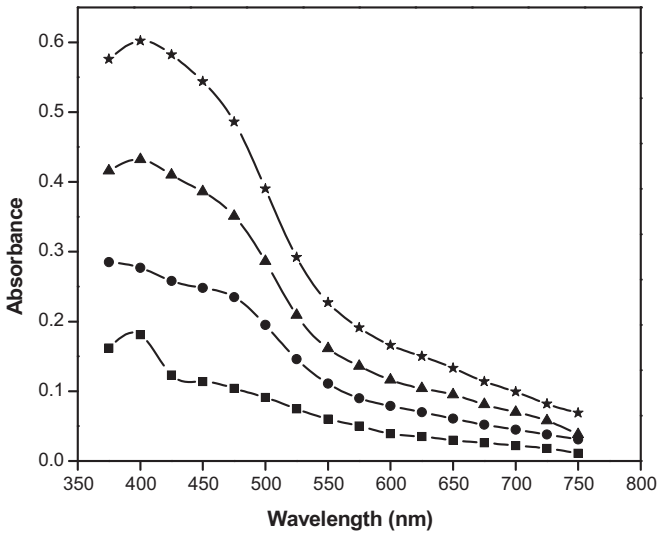

Fig. 1. Time-resolved UV–vis spectra of silver sol. *Reaction conditions*: [Ag^+] = 16.0×10^{-4} mol dm^{-3}; [CTAB] = 10.0×10^{-4} mol dm^{-3}; [aniline] = 40.0×10^{-4} mol dm^{-3}; temperature = 33 °C; time = 30 min (■), 60 min (●), 90 min (▲) and 120 min (*).

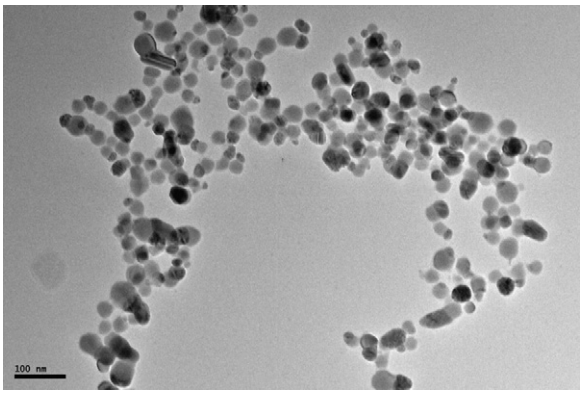

Fig. 2. TEM images of CTAB-stabilized Ag-nanoparticles. *Reaction conditions*: [Ag(I)] = 16.0×10^{-4} mol dm^{-3}; [CTAB] = 10.0×10^{-4} mol dm^{-3}; [aniline] = 20.0×10^{-4} mol dm^{-3}.

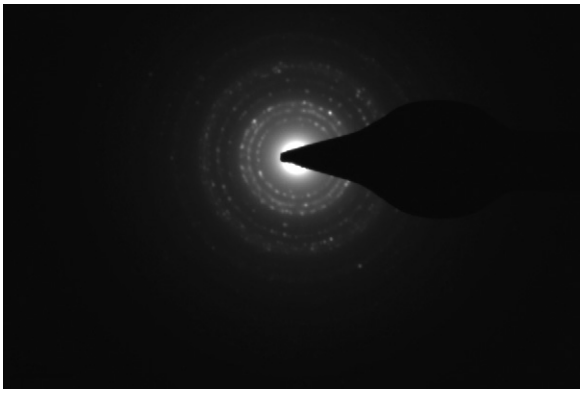

Fig. 3. SADE images of randomly selected Ag-nanoparticles of Fig. 2.

spherical Ag-nanoparticles and not hexagonal close-packed arrays and nanorods of Ag nanocrystals as these might have been synthesized in presence of aniline by the reduction of Ag^+ ions with hydrazine and citrate, respectively [30].

The selected area electron diffraction pattern of Ag nanoparticles is shown in Fig. 3. When the electron diffraction is carried out on a limited number of crystals one observes only some spots of diffraction distributed on concentric circles. The rings patterns are consistent with the plane families {1 1 1}, {2 0 0}, {2 2 0}, {3 1 1} and {3 3 1} of pure face-centred cubic silver structure [37].

3.2. Kinetic analysis of Ag-nanoparticles formation

Fig. 4 suggests that autocatalysis is involved in the silver sol formation. It was noted that the extent of deviation depended not only on [Ag^+] but also on [aniline] (Fig. 4). In the present study it

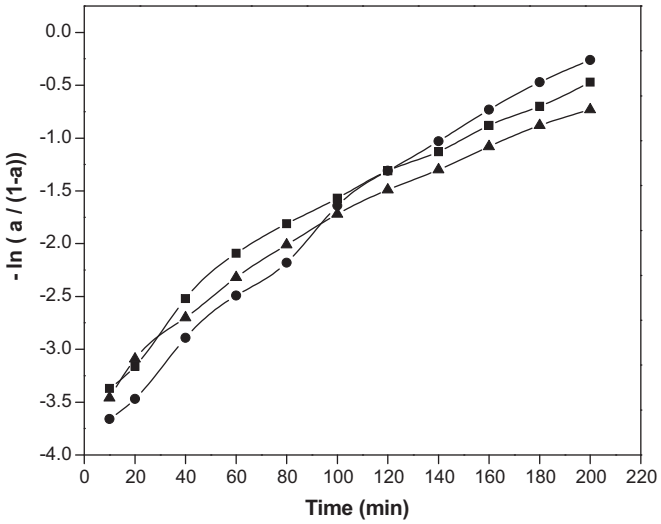

Fig. 4. Plot between $\log(a/(1-a))$ *versus* time for the formation of silver sol. *Reaction conditions*: [Ag^+] = 16.0×10^{-4} mol dm^{-3}; [CTAB] = 10.0×10^{-4} mol dm^{-3}; temperature = 33 °C; [aniline] = 30.0×10^{-4} mol dm^{-3} (●), 40.0×10^{-4} mol dm^{-3} (▲) and 20.0×10^{-4} mol dm^{-3} (■).

is necessary to point out that the plots of $\ln[a/(1-a)$ against time deviates from the linearity (Fig. 4), where $a = A_t/A_\alpha$ and A_t and A_α are the absorbances at times t and α, respectively [12,29]. The values of apparent rate constants were determined from the slopes of $\ln[a/(1-a)$ *versus* time plots (Table 1).

The effect of [Ag^+] on the rate of silver nanoparticles formation was studied at constant [aniline] (40.0×10^{-4} mol dm^{-3}), [CTAB] (10.0×10^{-4} mol dm^{-3}), and temperature (33 °C). k_{obs} values were found to be $6.5 \pm 0.1 \times 10^{-4}$ s^{-1} at [Ag^+] values of 4.0, 8.0, 12.0, 16.0 and 20.0×10^{-4} mol dm^{-3}. At lower [CTAB] (<4.0×10^{-4} mol dm^{-3}), the reaction mixtures becomes turbid and a gray precipitate appears where as, the formation of stable yellow color is observed in [CTAB] (≥6.0×10^{-4} mol dm^{-3}). On the other hand, transparent silver sol was not formed at higher [CTAB] (≥16.0×10^{-4} mol dm^{-3}) due to the dilution effect.

3.3. Mechanism of the reduction of Ag^+ ions by aniline

Tondre et al. [38] advised to avoid the use of even buffer solutions to maintain pH of micellar solutions. Control of pH is not as straightforward in micellar solutions as in ordinary solvents [39]). However, a series of experiments were also performed in order to see any change in the macroscopic pH of the working solution in presence of [aniline] and/or [CTAB]. The pH values was found to be nearly constant with increasing [CTAB] and [aniline] (weak base $K_b = 4.6 \times 10^{-10}$). The observed values of pH are given in Table 1. Therefore, it should be emphasized here that preparation of silver sols were studied with out adding acidifying- and buffering-agents.

Table 1
Values of pH and second-order rate constants and as a function of [aniline] and [CTAB] for the CTAB stabilized Ag-nanoparticles formation.

[Aniline] ($\times 10^{-4}$ mol dm^{-3})	[CTAB] ($\times 10^{-4}$ mol dm^{-3})	[Ag^+] ($\times 10^{-4}$ mol dm^{-3})	pH	k_{obs} ($\times 10^2$ mol dm^{-3})
10.0	60	16.0	10.3	25.2
20.0			10.2	44.0
30.0			10.4	10.6
40.0			10.3	6.5
50.0			10.5	6.2
60.0			10.4	5.6
40.0	6.0	16.0	10.3	6.7
	10.0		10.4	6.5
	16.0		10.5	Turbid
	24.0		10.4	Turbid
	30.0		10.3	Turbid

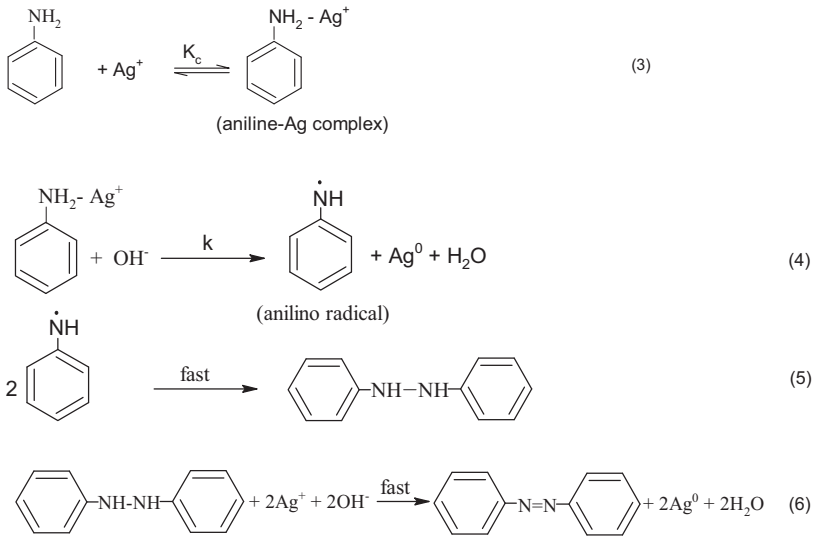

Scheme 1. Mechanism to the oxidation of aniline by Ag^+ ions.

It is well known that aniline participates in the following acid–base equilibrium:

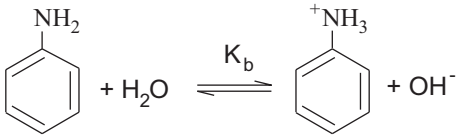

(1)

For which we can write expression (2)

$$pK_b = pH + \log\frac{[Ph\text{–}NH_2]}{[Ph\text{–}\overset{+}{N}H_3][OH^-]} \quad (2)$$

Under our experimental conditions, aniline is mainly present in the basic form and as the $[OH^-]$ increases the percentage of non-protonated species of aniline ($Ph\text{–}NH_2$) increases which in turn, increases the reaction rate. It is well known that there is no relationship between the oxidizing power of an oxidizing agent and the nature of the products obtained when aniline undergoes oxidation [40]. Before attempting to propose a mechanism for the silver sol formation, it is necessary to know the chemical speciation of silver(I) in presence of aniline. The standard electrode potential of Ag^+/Ag^0 redox couple is 0.799 V [40,41]. Generally, complexation decreases the redox potential and hence the reducibility of Ag^+ ions (redox potentials are 0.07, 0.24 and 0.37 V, respectively, for AgBr, AgOH and $[Ag(NH)_2]^+$). When Ag^+ ions were added in an aniline solution, the Ag^+ ions strongly bound to aniline by complex formation with the nucleophilic $–NH_2$ group (Scheme 1).

In Scheme 1, Eq. (3) represents the formation of a complex between Ag^+ and aniline. The reducibility of this complex strongly depended on the binding strength. The phenyl group is electron withdrawing. Thus, a large positive charge resides on the nitrogen atom, deactivating it for complexation. This accounts for the non-availability of the electron pairs at the seat of the reaction, i.e., complexation with Ag^+, and prevent the strong interactions between aniline and Ag^+ ions. By analogy with the previous observations [42], we assume that aniline–Ag complex decomposes in a one-step one-electron oxidation-reduction mechanism to Ag^0 and anilino radical (Eq. (4); rate determining step). After the slow electron transfer step, reactions (5) and (6) may follow. The proposed mechanism is further supported by the detection of radical with acrylonitrile and analysis of product formation with the IR (FT-IR spectra of the silver sol were also measured at the end of the reaction. A peak band appears at around 1575 cm^{-1} which is assigned to –N=N– group), azobenzene was identified as the oxidation product by comparison its FT-IR spectra against an authentic samples of azobenzene.

3.4. Role of aniline and probable reaction site

To confirm the role of aniline in the Ag-nanoparticles formation, the rate constant is plotted against the [aniline] (Fig. 5). Interestingly, the k_{obs} decreased from 44.0×10^{-4} s^{-1} to 5.6×10^{-2} mol^{-1} dm^3 s^{-1} with increasing [aniline]. These results may be interpreted by considering that the [Ag–aniline] complex, would increase when the [aniline] increases because of the presence of lone-pair of electrons on the amino group. As a results, the oxidation potential of Ag^+/Ag^0 couple decreases which, in turn, decreases the reduction rate of Ag^+ ions and subsequently agglomeration of Ag atoms during the reduction process. In addition, such type of behavior may also be explained in terms of adsorption of aniline onto the surface of metallic silver particles [11]. It can now be stated confidently that the rate of Ag-nanoparticles formation is

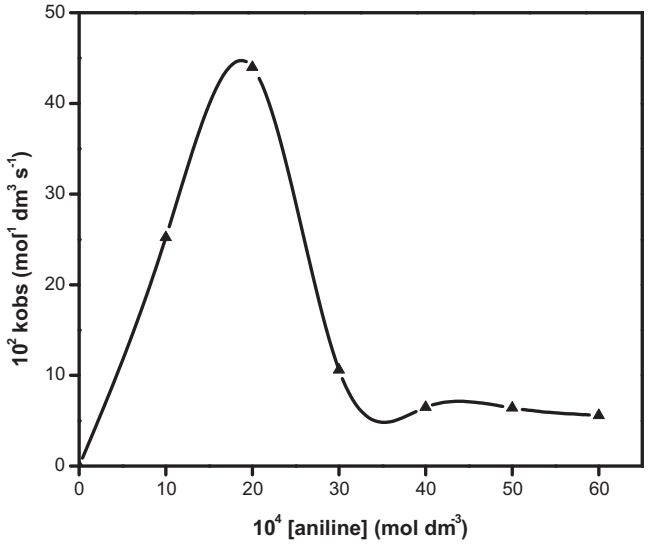

Fig. 5. Plot showing the effects of [aniline] on the second-order rate constants. *Reaction conditions*: $[Ag^+] = 16.0 \times 10^{-4}$ mol dm^{-3}; $[CTAB] = 10.0 \times 10^{-4}$ mol dm^{-3}; temperature = 33 °C.

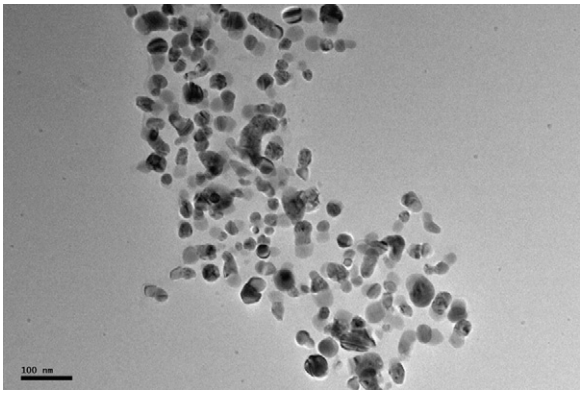

Fig. 6. TEM images of CTAB-stabilized Ag-nanoparticles. *Reaction conditions*: [Ag(I)] = 16.0×10^{-4} mol dm^{-3}; [CTAB] = 10.0×10^{-4} mol dm^{-3}; [aniline] = 50.0×10^{-4} mol dm^{-3}.

not directly proportional to the [aniline] (only small [aniline] being enough to initiate the formation of metal nucleation center which acts as a catalyst for the reduction of other Ag^+ present in the solution). On the other hand, cationic micelles of CTAB concentrates the reactants (Ag^+ ions and aniline), intermediate (Ag–aniline complex) and Ag-nanoparticles into the Stern-layer through hydrophobic and Van der Waals forces. No significant changes in the shape, size and the size distribution of Ag-nanoparticles were observed at [aniline] = 50.0×10^{-4} mol dm^{-3} (Fig. 6).

4. Conclusions

We have presented a new method for the preparation of CTAB stabilized Ag-nanoparticles with mean diameters of 10–30 nm based on the reduction of Ag^+ ions by aniline. The resulting nanoparticles solution displays the characteristic plasmon absorption band for spherical nanoparticles at 400 nm. TEM and selected area electron diffraction (SAED) confirmed that formation of spherical, aggregated and face-centered-cubic Ag-nanoparticles, respectively. The kinetics of nanoparticles formation was found to be extremely slow. We established that reduction rates of Ag^+ ions decreases with increasing [aniline]. Our results suggest that shape, size and the size distribution of the Ag-nanoparticles are not altered significantly with [aniline].

References

[1] Y. Sun, Y. Xia, Science 298 (2002) 2176.
[2] D. Yu, V.W.-W. Yam, J. Am. Chem. Soc. 126 (2004) 13200.
[3] D. Yu, V.W.-W. Yam, J. Phys. Chem. B 109 (2005) 5497.
[4] S.D. Solomon, M. Bahadory, A.V. Jeyarajasingam, S.A. Rutkowsky, C. Boritz, J. Chem. Educ. 84 (2007) 322.
[5] H. Won II., H. Nersisyan, C.W. Won, J.-M. Lee, J.-S. Hwang, Chem. Eng. J. 156 (2010) 459.
[6] S. Link, M.A. El-Sayed, J. Phys. Chem. B 103 (1999) 8410.
[7] I. Sondi, B. Salopek-Sondi, J. Colloid Interface Sci. 275 (2004) 177.
[8] S. De, A. Pal, N.R. Jana, T. Pal, J. Photochem. Photobiol. A: Chem. 131 (2000) 111.
[9] S.T. Dubas, V. Pimpan, Talanta 76 (2008) 29.
[10] V.K. Sharma, R.A. Yngard, Y. Lin, Adv. Colloid Interface Sci. 145 (2009) 83.
[11] A. Henglein, J. Phys. Chem. 97 (1993) 5457.
[12] Z.-Y. Huang, G. Mills, B. Hajek, J. Phys. Chem. 97 (1993) 11542.
[13] T. Pal, T.K. Sau, N.R. Jana, J. Colloid Interface Sci. 202 (1998) 30.
[14] W. Yan, R. Wang, Z. Xu, J. Xu, L. Lin, Z. Shen, Y. Zhou, J. Mol. Catal. A: Chem. 255 (2006) 81.
[15] S.A. Al-Thabaiti, F.M. Al-Nowaiser, A.Y. Obaid, A.O. Al-Youbi, Z. Khan, Colloids Surf. B: Biointerfaces 67 (2008) 230.
[16] A. Henglein, Chem. Rev. 89 (1989) 1861.
[17] M.A. El-Sayed, Acc. Chem. Res. 34 (2001) 257.
[18] Y. Huang, Y. Lin, H. Chang, Nanotechnology 17 (2006) 4885.
[19] W. Zhang, X. Qiau, J. Chen, Colloids Surf. A: Physicochem. Eng. Aspects 299 (2007) 22.
[20] Z. Khan, A. Talib, Colloid Surf. B: Biointerfaces 76 (2010) 164.
[21] I. Pastoriza-Santos, L.M. Liz-Marzan, Pure Appl. Chem. 72 (2000) 83.
[22] R. Patakfalvi, Z. Viranyi, I. Dekany, Colloid Polym. Sci. 283 (2004) 299.
[23] M. Kim, J.-W. Byun, D.-S. Shin, Y.-S. Lee, Mater. Res. Bull. 44 (2009) 334.
[24] E. Janata, A. Henglein, B.G. Ershov, J. Phys. Chem. 98 (1994) 10888.
[25] A. Henglein, Ber. Bunsen-Ges, Phys. Chem. 101 (1997) 1562.
[26] S. Gomez, K. Philippot, V. Collière, B. Chaudret, F. Senocq, P. Lecantec, Chem. Commun. (2000) 1945.
[27] L. Balogh, D.A. Tomalia, J. Am. Chem. Soc. 120 (1998) 7355.
[28] M. Zhao, L. Sun, R.M. Crooks, J. Am. Chem. Soc. 120 (1998) 4877.
[29] K. Esumi, T. Hosoyo, A. Yamahira, K. Torigoe, J. Colloid Interface Sci. 226 (2000) 346.
[30] Y. Tan, Y. Li, D. Zhu, J. Colloid Interface Sci. 258 (2003) 244.
[31] United States Environmental Protection Agency, OPPT Chemical Fact Sheets, Aniline Fact Sheet, Support Document (CAS No. 62-53-3), December 1994.
[32] K.C. Picel, V.C. Stamoudis, M.S. Simmons, Water Res. 22 (1988) 1189.
[33] C.D. Lyons, S. Kartz, R. Bartha, Appl. Environ. Microbiol. 48 (1984) 491.
[34] J. Sarasa, S. Cortés, P. Ormad, R. Gracia, J.L. Ovelleiro, Water Res. 36 (2002) 3035.
[35] P. Piccinini, C. Minero, M. Vincenti, E. Pelizzetti, J. Chem. Soc., Faraday Trans. 93 (1997) 1993.
[36] S.W. Heinzman, B. Gamen, J. Am. Chem. Soc. 104 (1982) 6801.
[37] M.G. Guzman, J. Dille, S. Godet, World Acad. Sci. Eng. Technol. 43 (2008) 357.
[38] R. Cierpiszewski, M. Hebrant, J. Szymanowski, C. Tondre, J. Chem. Soc. Faraday Trans. 92 (1996) 249.
[39] R. Bacaloglu, C.A. Bunton, J. Phys. Chem. 93 (1989) 1497.
[40] A.K. panda, S.N. Mahapatro, G.P. Panigrahi, J. Org. Chem. 46 (1981) 40000; D.V. Goia, E. Matijevic, New J. Chem. (1998) 1203.
[41] J. Xie, J.Y. Lee, D.I.C. Wang, Y.P. Ting, ACS Nano 1 (2007) 429.
[42] S.A. Al-Thabaiti, F.M. Al-Nowaiser, A.Y. Obaid, A.O. Al-Youbi, Z. Khan, Colloids Surfs. B: Biointerfaces 73 (2009) 284.